การศึกษาเชิงตัวเลขของการแข็งตัวของโลหะผสมในช่วงเริ่มต้นโดยใช้วิธีการแปลงแบบซิมมิลาร์ลิตี้และเทคนิคของซีแคนท์

A Numerical Study of an Early Stage of Alloy Solidification Using Similarity Transformation and Secant Iterative Technique

Chittin TANGTHIENG

Department of Mechanical Engineering, Faculty of Engineering, Chulalongkorn University,

Pyathai Road, Patumwan, Bangkok, 10300, Thailand

Tel : 0-2218-6590, Fax : 0-2218-6642, E-mail fmectt@eng.chula.ac.th

Abstract

An asymptotic case of alloy solidification is theoretically and numerically studied in this paper. In an early stage of alloy solidification, the problem is assumed one-dimensional and transient. The governing equations for four separate regions, i.e., wall, solid, mushy, and liquid regions, are formulated. A supplement equation representing an explicit expression between the solid fraction and the local temperature is incorporated to close the governing system. Similarity variables are introduced to transform the governing equations to a set of ordinary differential equations. A combination of the fourth-order Runge-Kutta and the Secant iterative technique is employed to obtain the solutions. Physical properties of the Pb-10 % wt Sn alloy as a solidified material and of the carbon steel as a wall material are used as a test case. Grid independence of the numerical results is examined. The solidus and liquidus constants, which represent the primary unknowns of the problem, and the temperature profile are determined.

บทคัดย่อ

บทความฉบับนี้ได้เสนอถึงการแก้ไขปัญหาการแข็งตัวของโลหะผสมในช่วงเริ่มต้นโดยระเบียบวิธีเชิงตัวเลข ในการศึกษาครั้งนี้จะตั้งสมมติฐานว่าปัญหานั้นเป็นแบบหนึ่งมิติและขึ้นกับเวลา สมการกำกับได้ถูกกำหนดขึ้นในบริเวณสี่แบบ ได้แก่ ผนัง ของแข็ง ของผสม(Mushy) และของเหลว นอกจากสมการกำกับแล้วยังรวมไปถึงสมการช่วยเหลือซึ่งแสดงถึงความสัมพันธ์ระหว่างอัตราส่วนของแข็ง(solid fraction) และอุณหภูมิ สมการกำกับในทั้งสี่โดเมนจะถูกเปลี่ยนให้อยู่ในรูปของระบบสมการเชิงอนุพันธ์สามัญโดยวิธีซิมมิลาร์ลิตี้ คำตอบของระบบสมการหาได้จากระเบียบวิธีรุงเง-กัตตา ลำดับที่สี่และวิธีการคำนวณซ้ำแบบซีแคนท์ ในการคำนวณเราใช้โลหะผสมของตะกั่วและพลวงโดยมีน้ำหนักพลวงอยู่ 10 % เป็นโลหะหลอมเหลว และใช้เหล็กกล้าเป็นแบบหล่อ ดังนั้นค่าพารามิเตอร์ต่าง ๆ สามารถหาได้จากคุณสมบัติเชิงความร้อนของวัสดุดังกล่าว นอกจากนั้นคำตอบเชิงเลขที่ได้จะถูกตรวจสอบถึงความเป็นอิสระต่อขนาดของกริดที่ใช้ ผลลัพธ์ที่นำเสนอจะอยู่ในรูปของค่าคงที่โซลิดัส และลิควิดัส และกราฟการเปลี่ยนแปลงของอุณหภูมิ

1. Introduction

For the past decades, many mathematical models for alloy solidification have been developed by many researchers using either the mixture theory [1,2] or the volume-average approach [3]. It is known that the difficulty of how to develop these mathematical models stems from the complexity of the mushy region, in which the solid and liquid can coexist in equilibrium over a range of temperature. In addition, the characteristic length scale of the solid structure surrounding by the liquid phase (i.e., dendrites) is on the order of 10^{-5} to 10^{-4} m, which is so small that the direct numerical simulation is not plausible. As a result, the average procedure must be employed to the governing equation, leading to unknown quantities needed to be modeled to close the governing system. These supplementary models include the expression of the solid fraction [4], the viscosity model [5], the expression for the interfacial terms [3], and more sophisticated microscopic models [6].

In general, the mathematical models are well suited for the finite-difference or the finite-element based algorithm. However, for an asymptotic case where the system can be simplified to a one-dimensional and transient problem, the similarity solution can be obtained rather than solving the finite-difference/volume equations. A major advantage of the similarity approach prior to the finite-difference/volume method is to reduce the computational time by collapsing two independent variables into one. In this study, the governing equations of an asymptotic case will be transformed to a set of similarity equations. The thickness of the solidified layer and the liquidus isotherm can be written in terms of the solidus and liquidus constants. The similarity equations can be solved by the fourth-order Runge-Kutta, together with the Secant iterative technique. Both of the solidus and liquidus constants and the variation of the temperature with the independent similarity variable are determined.

2. Problem Formulation

A schematic of the asymptotic case under consideration is depicted in Figure 1.

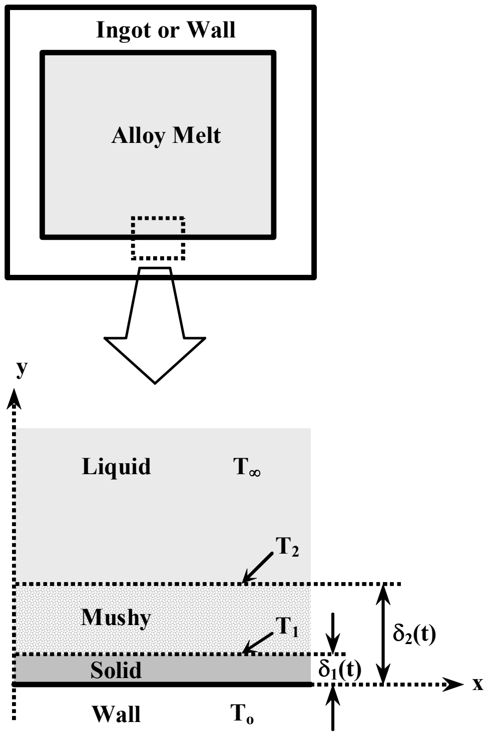

Figure 1 Schematic of the System under Consideration

In the early stage of solidification, the solidified layer is relatively thin compared to the thickness of the wall and to the characteristic length scale of the system. Therefore, the problem can be assumed one-dimensional and transient. In Figure 1, T_o and T_∞ represent the initial wall temperature and the initial melt temperature. T_1 and T_2 are the solidus and liquidus temperature of the binary alloy at a given composition. δ_1 and δ_2 represent the locations corresponding to T_1 and T_2, respectively. Note that the value of δ_1 is also equal to thickness of the solidified layer. The region bound between δ_1 and δ_2 is the mushy region, where the solid fraction, ε, is equal to unity at y = δ_1 and decreases to zero at y = δ_2.

To formulate the governing equations, a number of assumption must be made: (i) The system is one dimensional and transient. (ii) The wall is assumed semi-infinite. (iii) Physical properties of each phase are constant. (iv) In the early stage of solidification, convection in the liquid and mushy regions is negligible. (v) Local thermodynamics equilibrium exists. Thus, the solid fraction can be directly determined from the equilibrium phase diagram. (vi) Macrosegregation is assumed negligible.

It was found that the effects of the change of the density and the specific heat within the mushy region were small compared to that of the thermal conductivity [7]. Hence the density and the specific heat of the solid, liquid, and mushy regions are treated to be identical. On the other hand, the thermal conductivity of the mushy region is defined by taking an average of the thermal conductivity of each individual phase [1]:

$$k_m = (1-\varepsilon)\, k_\ell + \varepsilon\, k_s \tag{1}$$

With the aforementioned assumptions, the governing equations with associated boundary conditions for each region can be written as follows:

(i) Wall region

$$\rho\, c_p \frac{\partial T_w}{\partial t} = k_w \frac{\partial^2 T_w}{\partial y^2} \tag{2}$$

$$t = 0 : T_w = T_o \tag{3-a}$$

$$y = 0 : T_w = T_s \quad \text{and} \quad k_w \frac{\partial T_w}{\partial y} = k_s \frac{\partial T_s}{\partial y} \tag{3-b}$$

$$y \to -\infty : T_w = T_o \tag{3-c}$$

(ii) Solid region

$$\rho\, c_p \frac{\partial T_s}{\partial t} = k_s \frac{\partial^2 T_s}{\partial y^2} \tag{4}$$

$$t = 0 : \delta_1 = 0 \tag{5-a}$$

$$y = 0 : T_s = T_w \quad \text{and} \quad k_s \frac{\partial T_s}{\partial y} = k_w \frac{\partial T_w}{\partial y} \tag{5-b}$$

$$y = \delta_1 : T_s = T_1 \quad \text{and} \quad \frac{\partial T_s}{\partial y} = \frac{\partial T_m}{\partial y} \tag{5-c}$$

(iii) Mushy region

$$\rho\, c_p \frac{\partial T_m}{\partial t} = \frac{\partial}{\partial y}\left(k_m \frac{\partial T_m}{\partial y} \right) + \rho\, \Delta H \frac{\partial \varepsilon}{\partial t} \tag{6}$$

$$t = 0 : \delta_2 = 0 \tag{7-a}$$

$$y = \delta_1 : T_m = T_1 \quad \text{and} \quad \frac{\partial T_m}{\partial y} = \frac{\partial T_s}{\partial y} \tag{7-b}$$

$$y = \delta_2 : T_m = T_2 \quad \text{and} \quad \frac{\partial T_m}{\partial y} = \frac{\partial T_\ell}{\partial y} \tag{7-c}$$

(iv) Liquid region

$$\rho c_p \frac{\partial T_\ell}{\partial t} = k_\ell \frac{\partial^2 T_\ell}{\partial y^2} \tag{8}$$

$$t = 0 : T_\ell = T_\infty \tag{9-a}$$

$$y = \delta_2 : T_\ell = T_2 \ , \ \text{and} \quad \frac{\partial T_\ell}{\partial y} = \frac{\partial T_m}{\partial y} \tag{9-b}$$

$$y \to \infty : T_\ell = T_\infty \tag{9-c}$$

To close the governing system, the solid fraction must be specified in terms of the local temperature of the mushy region. In this study, the category of alloy solidification is limited to the isomorphous system where both constituents of the binary alloy are completely miscible in both liquid and solid phases. In addition, the liquidus and solidus lines are assumed to be straight lines as shown in Figure 2 [8].

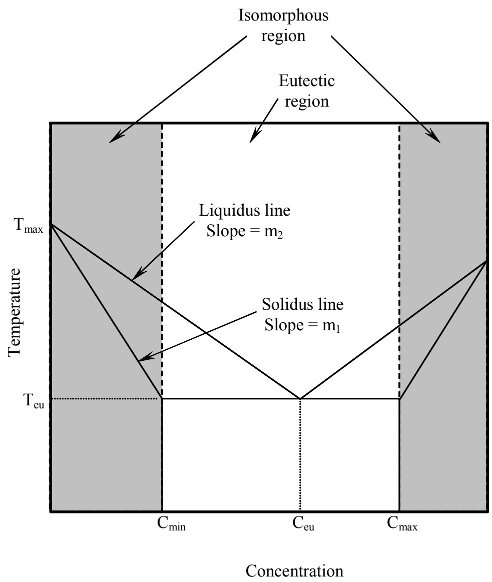

Figure 2 Simplified Equilibrium Phase Diagram

The relation between the solid fraction and the temperature is generally determined by applying the lever rule to the binary phase diagram, which is given by

$$\varepsilon = \frac{T_2 - T_m}{(T_2 - T_m) + \kappa (T_m - T_1)} \tag{10}$$

3. Mathematical Analysis

The governing equations (2)-(9) are transformed to the system of ordinary differential equations by introducing the similarity variables as follows:

(i) Wall region

$$\eta_w = \frac{y}{\sqrt{\alpha_w t}} \ ; \quad -\infty \le \eta_w \le 0$$
$$\theta_w = \frac{T_w - T_o}{T_1 - T_o} \ ; \quad 0 \le \theta_w \le \theta_{w(0)} \tag{11}$$

(ii) Solid region

$$\eta_s = \frac{y}{\delta_1} \ ; \quad 0 \le \eta_s \le 1$$
$$\theta_s = \frac{T_s - T_o}{T_1 - T_o} \ ; \quad \theta_{w(0)} = \theta_{s(0)} \le \theta_s \le 1 \tag{12}$$

(iii) Mushy region

$$\eta_m = 1 + \frac{y - \delta_1}{\delta_2 - \delta_1} \ ; \quad 1 \le \eta_m \le 2$$
$$\theta_m = 1 + \frac{T_m - T_1}{T_2 - T_1} \ ; \quad 1 \le \theta_m \le 2 \tag{13}$$

(iv) Liquid region

$$\eta_\ell = 1 + \frac{y}{\delta_2} \ ; \quad 2 \le \eta_\ell \le \infty$$
$$\theta_\ell = 2 + \frac{T_\ell - T_2}{T_\infty - T_2} \ ; \quad 2 \le \theta_\ell \le 3 \tag{14}$$

The solidus and liquidus lines, i.e., δ_1 and δ_2, are defined as

$$\delta_1 = \sigma_1 \sqrt{\alpha_s t} \tag{15}$$

$$\delta_2 = \sigma_2 \sqrt{\alpha_s t} \tag{16}$$

where σ_1 and σ_2 are the solidus and liquidus constants, which are the primary unknowns of the problem. After performing the similarity transformation by substituting equations (11)-(16) into equations (2)-(9), the system of ordinary differential equations are

(i) Wall region

$$\theta_w'' + \frac{\eta_w}{2} \theta_w' = 0 \tag{17}$$

$$\eta_w = 0 : \theta_w = \theta_s \quad \text{and} \quad \theta_w' = \frac{R_1}{\sigma_1} \theta_s' \tag{18-a}$$

$$\eta_w \to -\infty : \theta_w = 0 \tag{18-b}$$

(ii) Solid region

$$\theta_s'' + \frac{\sigma_1^2 \eta_s}{2}\theta_s' = 0 \tag{19}$$

$$\eta_s = 0:\ \theta_s = \theta_w \quad \text{and} \quad \theta_s' = \frac{\sigma_1}{R_1}\theta_w' \tag{20-a}$$

$$\eta_s = 1:\ \theta_s = 1 \quad \text{and} \quad \theta_s' = \frac{\sigma_1}{\sigma_2 - \sigma_1}\frac{1}{R_2}\theta_m' \tag{20-b}$$

(iii) Mushy region

$$\theta_m'' + \left(\frac{R_3 - 1}{R_3\varepsilon + (1-\varepsilon)}\right)\left(\frac{\kappa}{\mathrm{Ste}\,[(2-\theta_m) + \kappa(\theta_m - 1)]^2}\right)(\theta_m')^2$$
$$+ \left(\frac{R_3}{R_3\varepsilon + (1-\varepsilon)}\right)\left(1 + \frac{\kappa}{\mathrm{Ste}\,[(2-\theta_m) + \kappa(\theta_m - 1)]^2}\right)$$
$$\times\left(\frac{(\sigma_2 - \sigma_1)^2}{2}\right)\left(\eta_m - 1 + \frac{\sigma_1}{\sigma_2 - \sigma_1}\right)\theta_m' = 0$$

(21)

$$\eta_m = 1:\ \theta_m = 1 \quad \text{and} \quad \theta_m' = \frac{\sigma_2 - \sigma_1}{\sigma_1}R_2\theta_s' \tag{22-a}$$

$$\eta_m = 2:\ \theta_m = 2 \quad \text{and} \quad \theta_m' = \frac{\sigma_2 - \sigma_1}{\sigma_2}R_4\theta_\ell' \tag{22-b}$$

(iv) Liquid region

$$\theta_\ell'' + R_3\frac{\sigma_2^2}{2}(\eta_\ell - 1)\theta_\ell' = 0 \tag{23}$$

$$\eta_\ell = 2:\ \theta_\ell = 2 \quad \text{and} \quad \theta_\ell' = \frac{\sigma_2}{\sigma_2 - \sigma_1}\frac{1}{R_4}\theta_m' \tag{24-a}$$

$$\eta_\ell \to \infty:\ \theta_\ell = 3 \tag{24-b}$$

The transformed supplementary equation (equation (10)) is

$$\varepsilon = \frac{2 - \theta_m}{(2-\theta_m) + \kappa(\theta_m - 1)} \tag{25}$$

The dimensionless parameters appearing in equations (17)-(25) are the solid-to-wall thermal ratio R_1, the wall subcooling parameter R_2, the solid-to-liquid thermal conductivity ratio R_3, the liquid superheating parameter R_4, the Stefan number Ste, and the equilibrium partition ratio κ. These parameters are defined as

$$R_1 = \sqrt{\frac{k_s\,\rho\,c_p}{k_w\rho_w c_{pw}}}\ ,\ R_2 = \frac{T_1 - T_o}{T_2 - T_1}\ ,\ R_3 = \frac{k_S}{k_\ell}$$
$$R_4 = \frac{T_\infty - T_2}{T_2 - T_1}\ ,\ \mathrm{Ste} = \frac{c_p(T_2 - T_1)}{\Delta H}\ ,\ \text{and}\ \kappa = \frac{m_2}{m_1} \tag{26}$$

4. Numerical Solution Procedure

Analytical solutions for θ_w and θ_s from equations (17) and (19) can be determined by direct integration, which are

$$\theta_w = \frac{R_1}{R_1 + \mathrm{erf}(\sigma_1/2)}\left[1 + \mathrm{erf}\left(\frac{\eta_w}{2}\right)\right] \tag{27}$$

$$\theta_s = \frac{R_1 + \mathrm{erf}\left(\frac{\sigma_1\eta_s}{2}\right)}{R_1 + \mathrm{erf}(\sigma_1/2)} \tag{28}$$

On the other hand, equations (21) and (23) must be solved numerically using the classical fourth-order Runge-Kutta method. The initial conditions are the values of θ_m and θ_m' at $\eta_m = 1$, which are given by equation (22-a). The value of θ_s' at $\eta_s = 1$ can be obtained by directly differentiating equation (28). Substituting $\theta_s'(1)$ into equation (22-a) yields

$$\theta_m'(1) = \frac{(\sigma_2 - \sigma_1)R_2}{\sqrt{\pi}}\left[\frac{\exp(-\sigma_1^2/4)}{R_1 + \mathrm{erf}(\sigma_1/2)}\right] \tag{29}$$

It can be seen that equation (29) are still a function of σ_1 and σ_2, which are unknowns of the problem. The values of σ_1 and σ_2 are estimated first. Then, the fourth-order Runge-Kutta method is performed by marching through η coordinate. Finally, the secant iterative technique is applied to update σ_1 and σ_2 until these two values match the boundary conditions, i.e., $\theta_m(2) = 2$ and $\theta_m(\infty) = 3$. The solution is shown to converge if the difference between the values of σ_1 and σ_2 and the matching conditions is less than a prescribed tolerance of 10^{-8}.

Note that although the solution of the governing equation for the liquid region, equation (23), can be analytically determined, it is very difficult to obtain a converging solution by numerically solving the governing equation for the mushy region, equation (21), alone. This is due to the fact that the matching conditions, equation (22-b), are still a function of σ_1 and σ_2.

In this study, the properties of the Pb-10 % wt Sn alloy and the carbon steel are used to calculated the controlling parameters appearing in equation (26) as a test case. The values of the properties are summarized in Table 1.

Table 1 Properties and data used to calculate the controlling parameters

Pb-10 % wt Sn alloy [9]
ρ = 10,100 kg/m^3
c_p = 167 J/(kg-K)
k_s = 15.6 W/(m-K)
k_ℓ = 15.9 W/(m-K)
ΔH = 26,000 J/kg
Carbon Steel [10]
ρ_w = 7,832 kg/m^3
c_{pw} = 434 J/(kg-K)
k_w = 63.9 W/(m-K)
Data from Pb-Sn phase diagram [11]
κ = 0.310
T_1 = 548 K
T_2 = 573 K
Controlling temperatures
T_o = 300 K
T_∞ = 650 K

According to the data given in Table 1, the controlling parameters are as follows:

$$R_1 = 0.348 \ , \ R_2 = 9.92 \ , \ R_3 = 0.985 \\ R_4 = 3.08 \ , \ \text{Ste} = 0.161 \ , \ \text{and} \ \kappa = 0.310 \tag{30}$$

5. Results and Discussion

Grid independence is examined by varying a number of grids in the mushy and liquid regions (N_m and N_ℓ, respectively). The result is depicted in Figure 3 below.

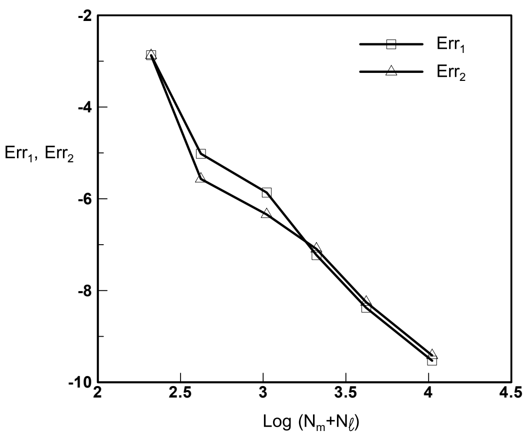

Figure 3 Variation of Relative Error with a Number of Grids

Err_1 and Err_2 are the relative errors for σ_1 and σ_2, respectively. The relative errors decrease as a number of grids is increased, resulting in the grid independence of the numerical results.

After the numerical procedure described earlier is performed, the values of σ_1 and σ_2 for a given set of controlling parameters in equation (30) can be obtained:

$$\sigma_1 = 0.761 \quad \text{and} \quad \sigma_2 = 0.970 \tag{31}$$

Thus, the variation of δ_1 and δ_2 as a function of time can be determined from equations (15) and (16), which can be graphically depicted in Figure 4.

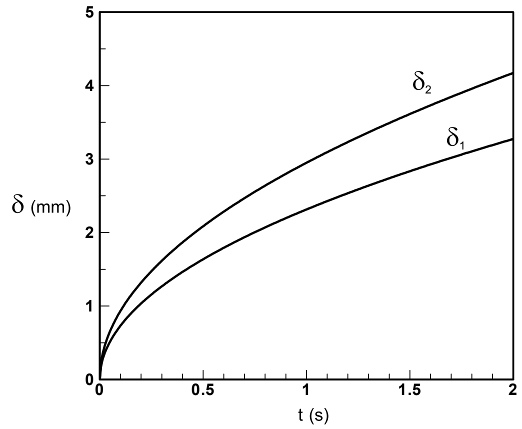

Figure 4 Variation of the Coating Thickness and the Liquidus Isotherm with time

It can be seen that both δ_1 and δ_2 grow monotonically due to the semi-infinite wall assumption. In addition, the thickness of the mushy layer, i.e. $\delta_1 - \delta_2$, is approximately 27 percent of the thickness of the solidified later, i.e., δ_1. It should be noted that as δ_1 and δ_2 get thicker, the ratio of the wall thickness to either δ_1 or δ_2 decreases as well. Therefore, the validity of the semi-infinite wall assumption should be carefully examined.

Figure 5 depicts the temperature profile across all regions in terms of the similarity variables. As expected, the temperature rises from the initial wall temperature toward the ambient melt temperature with increasing η. Note that in the solid and mushy regions, the temperature gradient becomes relatively large compared to the other two regions. Physically, the temperature increases at a further distance measured from the wall at an instant time. On the other hand, at a fixed location, the longer time the solidification takes, the lower the temperature will be. It can be seen that the temperature reaches the edge of the thermal boundary layer at η is approximately equal to 5. Beyond this location, the cooling front has not yet penetrated into the warm liquid.

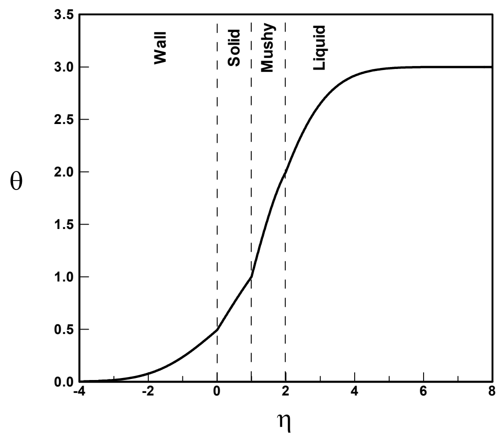

Figure 5 Temperature Profile of the Test Case

6. Conclusions

The theoretical and numerical study of an early stage of alloy solidification has been performed in this study. The paper also presents how to adapt the numerical technique to a phase-change problem by combining the similarity transformation, the fourth-other Runge-Kutta method, and the Secant iterative technique. The solidified layer and the liquidus isotherm can be written in terms of the solidification constants, which are equal to 0.761 and 0.970 for the test case.

Nomenclature

Symbols

c_p	=	specific heat [J/kg-K]
Err	=	relative error
ΔH	=	latent heat of freezing [J/kg]
k	=	thermal conductivity [W/m-K]
m	=	slope of a line in an equilibrium phase diagram
N	=	number of grids
R_1	=	solid-to-wall thermal ratio
R_2	=	wall subcooling parameter
R_3	=	solid-to-liquid thermal conductivity ratio
R_1	=	liquid superheating parameter
Ste	=	Stefan number
t	=	time [s]
T	=	temperature [K]
y	=	spatial coordinate [m]

Greek Symbols

α	=	thermal diffusivity [m^2/s]
δ	=	thickness [m]
ε	=	solid fraction
η	=	similarity independent variable
κ	=	equilibrium partition ratio
ρ	=	density [kg/m^3]
σ	=	solidification constant
θ	=	dimensionless temperature

Subscripts

o	=	initial state
1	=	corresponding to the solidus temperature
2	=	corresponding to the liquidus temperature
ℓ	=	liquid region
m	=	mushy region
s	=	solid region
w	=	wall region
∞	=	ambient state

References

[1] Bennon, W. D. and Incropera, F. P., "A Continuum Model for Momentum, Heat and Species Transport in Binary Solid-liquid Phase Change Systems-I. Model Formulation," Int. J .Heat Mass Transfer, Vol. 30, pp. 2161-2170, 1987.

[2] Voller, V. R., Brent, A. D., and Prakash, C., "The Modelling of Heat, Mass and Solute Transport in Solidification Systems," Int. J. Heat Mass Transfer, Vol. 32, pp. 1718-1731, 1989.

[3] Ni, J. and Beckermann, C., "A Volume-Averaged Two-Phase Model for Transport Phenomena during Solidification," Metall. Trans. B, Vol. 22B, pp. 339-361, 1991.

[4] Beckermann, C. and Viskanta, R., "Double-Diffusive Convection during Dendritic Solidification of a Binary Alloy," PhysicoChem. Hydrodyn., Vol. 10, pp. 195-213, 1988.

[5] Krieger, I. M., "Rheology of Monodisperse Lactices," Adv. Colloid. Interface Sci., Vol. 3, pp. 111-126, 1972.

[6] Wang, C. Y. and Beckermann, C., "Equiaxed Dendritic Solidification with Convection: Part I Multiscale/Multiphase Modeling," Metall. Mater. Trans. A, Vol. 27A, pp. 2754-2764, 1996.

[7] Stevens, R. and Poulikakos, D., "Freeze Coating of a Moving Substrate with a Binary Alloy," Numer. Heat Transfer Part A, Vol. 20, pp. 409-432, 1991.

[8] Kurz, W. and Fisher, D. J., Fundamentals of Solidification, 3rd edition, Trans Tech, Switzerland, pp. 15-16, 1989.

[9] Felicelli, S. D., Heinrich, J. C., and Poirier, D. R., "Simulation of Freckles During Vertical Solidification of Binary Alloys," Metall. Trans. B, Vol. 22B, pp. 847-859, 1991.

[10] Incropera, F. P. and Dewitt, D. P., Fundamentals of Heat and Mass Transfer, 5th edition, Wiley, New York, p 906, 2002.

[11] Massalski, T. B. (editor-in-Chief), Binary Alloy Phase Diagram, 2nd edition, Vol. 3, ASM International, Ohio, p. 3016, 1990.